NRIAG Journal of Astronomy and Geophysics (2015) **4**, 1–15

National Research Institute of Astronomy and Geophysics

NRIAG Journal of Astronomy and Geophysics

www.elsevier.com/locate/nrjag

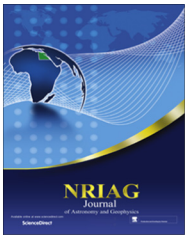

Early Cretaceous counterclockwise rotation of Northeast Africa within the equatorial zone: Paleomagnetic study on Mansouri ring complex, Southeastern Desert, Egypt

Hamza I. Lotfy

Department of Geology, Minia University, Egypt

Received 2 November 2014; revised 4 January 2015; accepted 13 January 2015
Available online 16 February 2015

KEYWORDS

Paleomagnetism;
Paleo-latitude;
Mansouri ring complex;
Africa;
Early Cretaceous paleomagnetic pole

Abstract The Mansouri ring complex (132 Ma) is, paleomagnetically, studied to shed light on the paleo-tectonic position of Northeast Africa during the Early Cretaceous. Progressive thermal demagnetization of all samples verified a general bi-vectorial decay of the natural remanence. After the removal of the present-day field overprint, the decaying anchored component was either:

1. A dual-polarity, shallow NW–SE directed component residing in magnetite (400–585 °C) of shiny fresh samples, or,
2. A normal-polarity, medium-inclination, north-oriented component stored in haematite of few reddish ferruginous sites. This component was considered as chemical remagnetization carried by secondary haematite.

Due to its steady stability, overwhelming existence in most sites, positive reversal test and its residence in fresh-samples' magnetite, the first dual-polarity, shallow NW–SE component, was considered as the characteristic remanent magnetization [ChRM] representing the paleomagnetic field during cooling of the Mansouri ring complex. The mean paleomagnetic pole of the isolated ChRM was at 47°N/259°E, Dp/Dm = 3.4°/6.6°.

This Hauterivian pole from Egypt shows reasonable consistency with its coeval poles rotated from the main tectonic units to Northeast Africa. It reveals that in Early Cretaceous:

1. Northeast Africa was equatorial, lying just south the Equator. Cairo, which is now at 30°N, was at −1.5° paleo-latitude.

E-mail address: Hiloutfy@yahoo.com

Peer review under responsibility of National Research Institute of Astronomy and Geophysics.

ELSEVIER **Production and hosting by Elsevier**

http://dx.doi.org/10.1016/j.nrjag.2015.01.001

2. The Azimuth of the African Plate was NE–SW, about 30° clockwise with respect to the present-day N–S trend.

Comparing this Hauterivian pole to that of the Wadi Natash basalts [107 ± 4 Ma], which was at [55°N/250°E] during the Albian, the African Plate seems to have rotated counter-clockwise about 10° with Northeast Africa moving northwards [Cairo was moving from 1.5°S to 1.5°N] within the equatorial zone, during the Early Cretaceous.

1. Introduction

In the Early Cretaceous, West Gondwana was suffering progressive fragmentation by the northward propagation of the South Atlantic rift between Africa and South America. During the Barremian, sea-floor spreading of the South Atlantic began from the south, concurrently, associated with reorganization of the Central Atlantic Ridge (Klitgord and Schouten, 1986; Savostin et al., 1986). Despite that the lithospheric extension was, certainly, underway in the Valanginian, the sea-floor spreading initiation was not earlier than 133 Ma ago (Rabinowitz and Labrecque, 1979), or slightly later between 130 and 125 Ma ago (Milner et al., 1995).

During its northward propagation, the South Atlantic created a North–South-oriented stress field in West and central Africa, reactivating the East–West-trending, Pan-African-aged, Central African Shear zone (Daly et al., 1989; Maurin and Guiraud, 1993). On top of the Central African shear zone, the African Plate was, deeply, fragmented by two rift systems: the equatorial East–West-trending Central African rift and the West African rift. These intra-plate rifts created impressive intra-plate deformations within Africa and plate rearrangement extending as far as the Indian Ocean (Wilson and Guiraud, 1992). The associated ocean-continent interaction provided concurrent widespread intra-plate extensional stresses evolving a system of East–West trending rifts interconnected by NW–SE trending strike-slip faults (Guiraud and Maurin, 1991, 1992), along which numerous, moderately, subsiding sedimentary basins with horst and graben structures evolved (Janssen et al., 1995) many of them are petroliferous.

Despite that the Valanginian drop in sea-level led to a general regression and scarcity of the Early Cretaceous sedimentary rocks, the associated intra-plate rifting within Africa created a phase of regional volcanic activity in Northeast Africa. This Early Cretaceous regional magmatic activity is marked in the Southeastern Desert of Egypt by the presence of frequent alkaline ring complexes (El-Reedy, 1979; Hashad and El-Reedy, 1979; Serencsits et al., 1979, 1981; Meneisy, 1990) in the northeastern Red Sea hills in Sudan (Klemenic, 1987; Semtner, 1993) and Israel (Lang et al., 1988; Lang and Steinitz, 1989; Garfunkel, 1992).

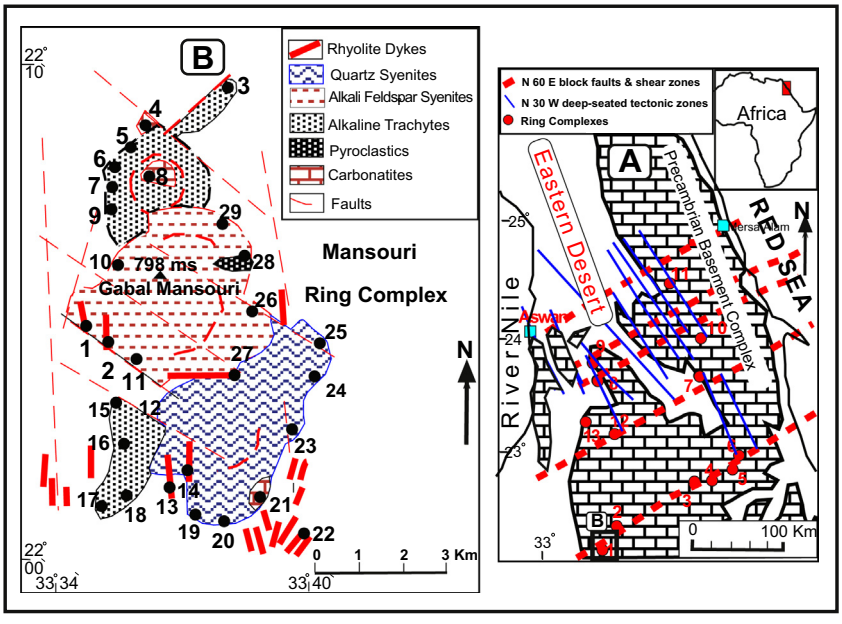

Fig. 1 (A) Distribution of the ring complexes in the Southeastern Desert of Egypt along the main tectonic fractures of the Precambrian basement complex (modified after Garson and Krs, 1976). Numbers denote the ring complexes: 1 – Mansouri, 2 – Gezira, 3 – Naga, 4 – Mishbeh, 5 – Nigrub El-Fogani, 6 – Nigrub El-Tahtani, 7 – Zargat Naam, 8 – Tarbtie South, 9 – Tarbtie North, 10 – Kahfa, 11 – Abu Kruq, 12 – Hadayib, and 13 – Um Risha. (B) Simplified geologic map of Mansouri ring complex (El-Nisr and Saleh, 2001) showing the main rock units along with the numbers and location of the sampling sites.

In the present paleomagnetic study, the multi-phase igneous rocks forming the Mansouri ring complex dated as 132 ± 10 Ma (El-Reedy, 1979; Hashad and El-Reedy, 1979; Meneisy, 1990), are studied to shed light on the paleo-tectonic position of the African Plate during the Early Cretaceous (Hauterivian) time, just before the fragmentation of West Gondwana by the South Atlantic Ocean and the drifting of Africa away from South America.

2. Geology of the Mansouri ring

The Mansouri ring complex [22.05°N–33.63°E] lies in the extreme southern part of the Egyptian Eastern Desert (Fig. 1A) and represents the southernmost ring complex in Egypt. The complex forms a sharp prominent hill measuring about 6 kms E–W and 9 kms N–S, protruding through country rocks composed of Precambrian metavolcanics, granodiorites and quartz-diorites.

The Mansouri ring is composed of a continuous main mass of variable alkali syenite rocks (including nordmarkite) intruding older remnants of cone volcanics, flows and a volcanic neck of trachyte, tuffs and pyroclastics. The main mass of the ring is nearly an isometric pluton of about 5 kms in diameter differentiated into alkali feldspar syenite and quartz-syenite (Fig. 1B). The whole complex is cut by frequent well-defined radial and ring dykes composed of hypabyssal alkali syenite porphyry, solvbergite with rhyolite cutting both the complex and the country rocks. The relics of the volcanic cone occupy the northern part of the complex with a chimney of alkaline trachyte surrounded by hypabyssal equivalents. The sequence of rock formation extends from the early eruption of alkali trachyte lavas with their pyroclastics and hypabyssal

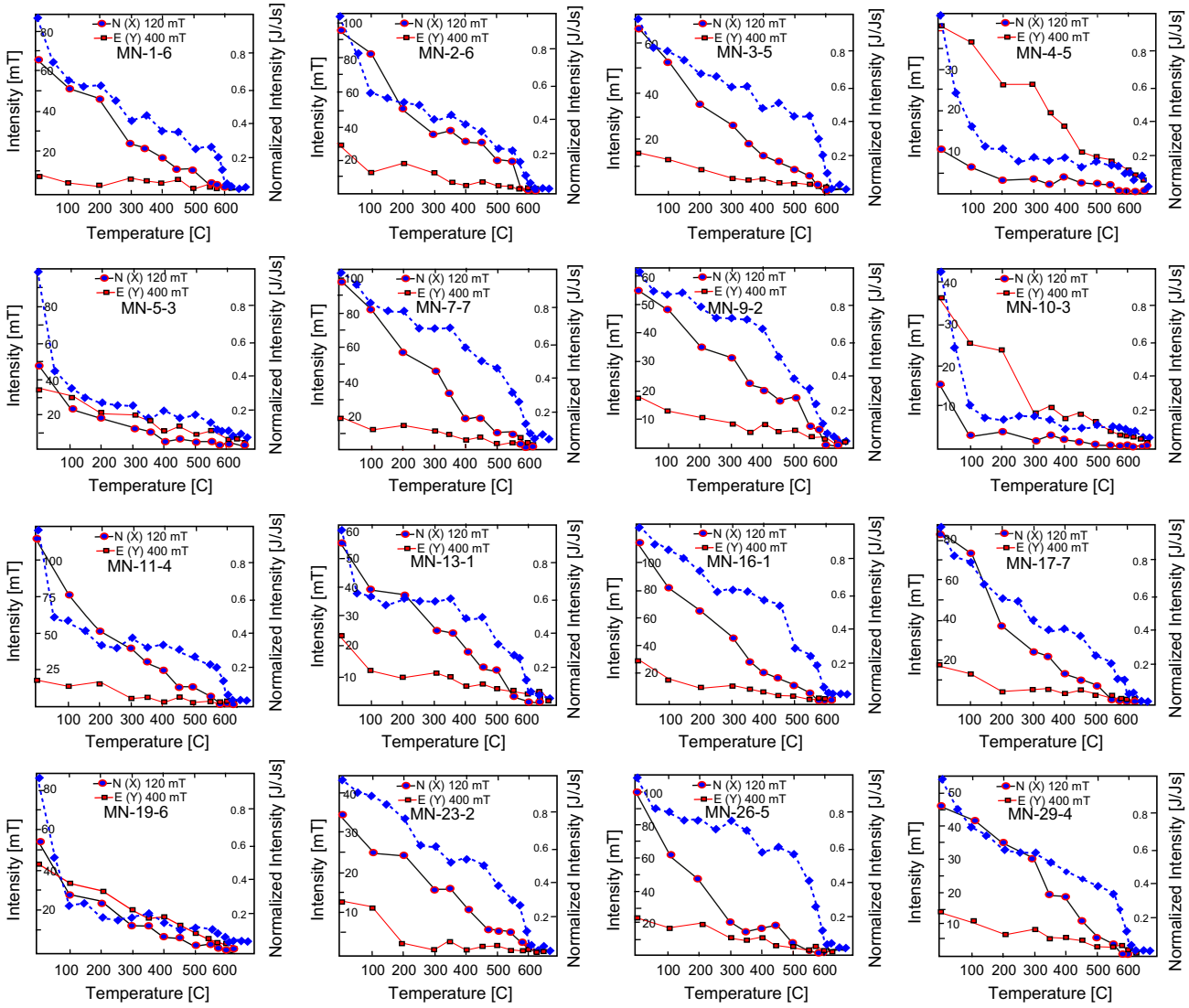

Fig. 2 Isothermal remanent magnetization [IRM] behavior of representative samples of the Mansouri ring complex. The rate of thermal decay of IRM intensity acquired along two perpendicular axes is presented on the left-hand scale. Lines joining the closed squares represent the decay of the 400 mT IRM acquired along the East [*Y*] axis reflecting the relative contribution of haematite. Lines connecting closed circles represent the decay of the 120 mT IRM acquired along the North [*X*] axis monitoring magnetite. The descending dashed lines joining closed diamonds represent the normalized thermal decay (right-hand scale) of the 800 mT IRM imparted in Mansouri samples.

equivalents covering the whole area, to the intrusion of various alkali syenitic rocks followed by the end phase of the ring and radial dykes (El Ramly et al., 1970, 1971).

It is worth mentioning, here, that the largest occurrence of carbonatite in Egypt is recorded in Mansouri complex (El Ramly et al., 1970, 1971). As the carbonatite rocks do not extend through the alkali syenite main mass, they are considered older than the main mass of the Mansouri ring complex (El Ramly and Hussein, 1982, 1985).

El-Nisr and Saleh (2001) stated that Mansouri complex was originated from mantle-derived magma with little crustal contamination in within-plate tectonic setting. They, also, referred the complex radioactive anomalies to the abnormal accumulations of U–Th bearing minerals associated with the E–W trending shear zones.

Structurally, the Mansouri complex seems, like other Egyptian ring complexes in the Eastern Desert, to be intimately connected with two sets of cross-cutting N30°W deep-seated tectonic zones and N60°E block faults and shear zones (Fig. 1A) (Garson and Krs, 1976).

Regarding the age of the Mansouri complex, its syenite yields Rb/Sr whole rock isochron age of 132 ± 10 Ma (El-Reedy, 1979; Hashad and El-Reedy, 1979; Meneisy, 1990). This date is an Early Cretaceous [Hauterivian] age according to Cohen et al. (2013) and Gradstein et al. (2012) geologic timescales.

3. Sampling

A number of twenty-nine sites were collected from the Mansouri ring complex rocks for paleomagnetic investigation. Sampling covered all rock-units from the oldest trachyte and pyroclastic flows passing through the main mass syenitic rocks [both the alkali-feldspar and quartz-syenite] till the youngest rhyolite dykes. The carbonatite exposures were, also,

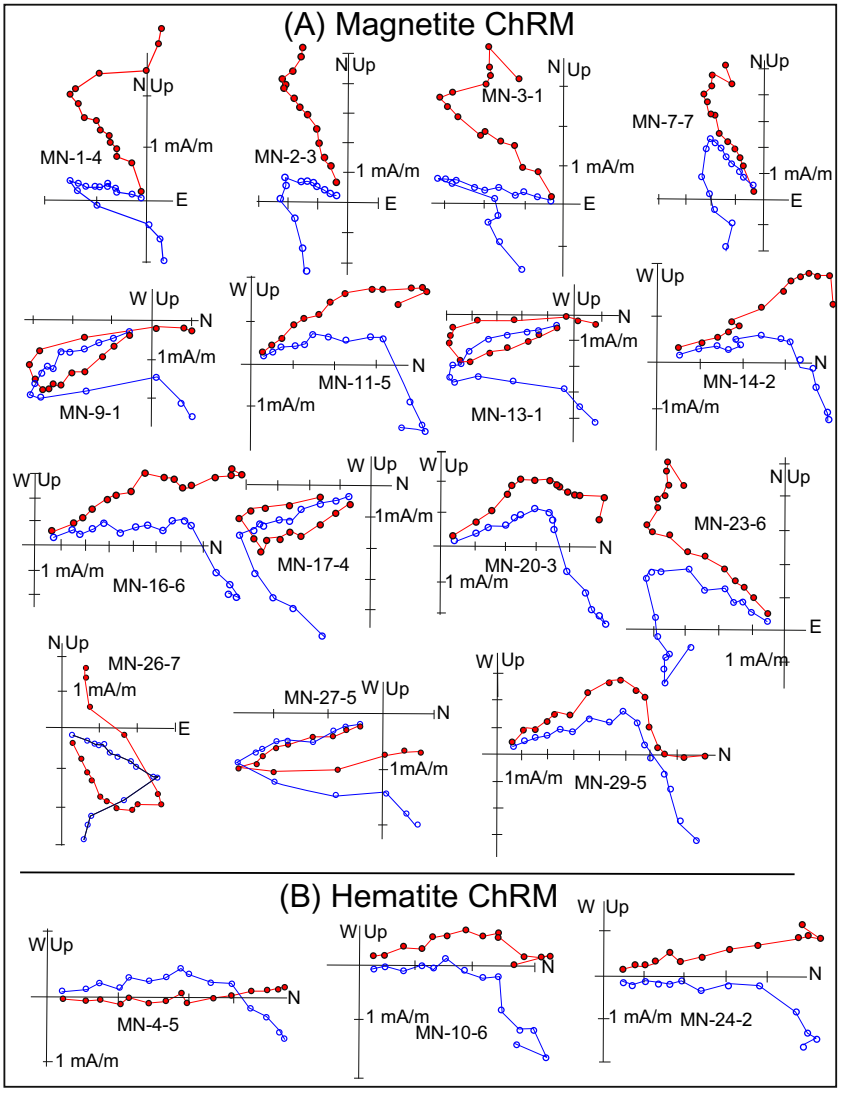

Fig. 3 Orthogonal projections (Zijderveld, 1967) of the demagnetization curves during progressive thermal demagnetization. A. Magnetite-dominated sites. B. Haematite-dominated sites. In the orthogonal projections, open circle (filled circle) projections denote the remanence decay in the vertical (horizontal) planes.

separately sampled. Due to the harsh topography, many sites were concentrated along the periphery with some sites collected from the inner deep gullies cutting the complex. Sites were distributed at different altitudes during the collection of the older volcanic flows. About 30 cm of weathered rocks were usually cleaned-off before sampling to avoid the weathered chemically-altered rocks. Due to the remoteness of Mansouri complex and the limited water supply required for the portable core drill, cores were, concurrently, collected with blocks. A number of 4–7 individually oriented cores and/or blocks were collected at each site using a solar compass for orientation.

4. Isothermal remanent magnetization [IRM] study

The paleomagnetic measurements, which were carried on an Agico JR-6 dual-speed spinner magnetometer [sensitivity 2×10^{-3} mA/m], thermal demagnetizer model [MMTD80], and Molspin magnetically-shielded alternating field demagnetizer, all housed in the Paleomagnetic Laboratory of the National Research Institute of Astronomy and Geophysics [NRIAG] in Egypt, included both the IRM study and the natural remanent progressive stepwise thermal demagnetization.

The IRM study was introduced to reveal the magnetic mineral association carrying the magnetic remanence in the collected sites. However, due the limited power of the available electromagnet, the IRM was applied in two successive schemes on twin samples selected from each site to verify the remanence carriers (Fig. 2).

1. First, a two-axis saturation magnetization was carried out through acquiring two different intensities of IRM along two different perpendicular axes [East and North] in the samples (Heller, 1978), followed by progressive stepwise thermal demagnetization up to 650 °C to monitor the thermal decay of the intensity [mT] of the imparted two perpendicular components of IRMs along their contiguous axes (along the vertical left-side scale in Fig. 2). The acquisition of 120 mT IRM along the North (X) axis is suitable to saturate magnetically soft magnetite expected to be the carrier of the primary characteristic remanence in the samples. On the other hand, an IRM of 400 mT was imparted along the East (Y) axis to saturate the magnetically harder haematite which, sometimes, carries secondary magnetization.
2. Subsequently, a twin sample from the same core was, then, saturated unidirectional up to 800 mT, then, thermally demagnetized up to 650 °C. The normalized intensity decay [J/Js] of this unidirectional IRM is presented by the dashed lines and monitored along the right-side scale in Fig. 2. This step was carried out to inspect the contribution of the low curie-temperature goethite, which is completely demagnetized below 150 °C and could retain only the present-day field overprint [PDF].

The inspection of the two-axis saturation magnetization decay curves (Fig. 2), reflects that both magnetite and haematite coexist with different contribution in most samples. Magnetite (the curves with circles), seems to be the main

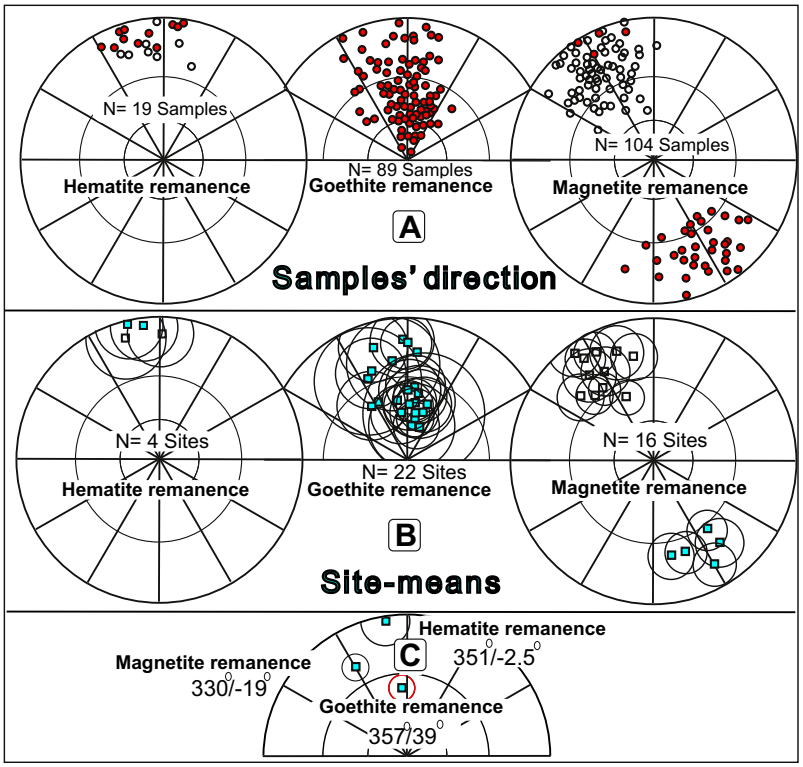

Fig. 4 Equal area projections showing the directions of the isolated demagnetized magnetic components in Mansouri Complex. In the upper part are the directions of the anchored haematite remanence > 585 °C [left projection], the direction of the PDF overprint carried by goethite (< 150 °C) [middle projection] and the direction of the anchored magnetite (ChRM) component [right projection], of all samples. In the central part are the site-means with their cones of 95% confidence of the three magnetic components. In the lower part are the respective overall ring-mean directions for the three isolated components. (N) denotes the number of samples (sites) included in the upper (central) projections.

Table 1 Paleomagnetic demagnetization results of Mansouri ring complex, N = number of demagnetized samples/sites, n = number of isolated directions/site, PDF = present-day field overprint, Mag. Car. = magnetic carrier, Dec. = declination [°], Inc. = inclination [°], K = kappa precision parameter (Fisher, 1953), α95[°] = the semi-angle of the 95% cone of confidence about the paleomagnetic pole (Fisher, 1953), VGP [°N/°E] = virtual geomagnetic North poles location, Dp/Dm = the semi-angle of the 95% cone of confidence about the paleomagnetic pole in the co-latitude direction (Dp) and at right-angle (Dm). Shaded sites are included in the haematite mean direction and paleomagnetic pole only as they are considered as secondary chemical magnetization.

Mansouri alkaline ring complex [22.05°N/33.63°E] [132 ± 10 Ma]										
Demagnetized sites/samples			Goethite component [PDF]				Anchored component			
Site	Rock type	N	n	Dec.°/Inc.°	K/α95°	Mag. Car.	n	Dec.°/Inc.°	K/α95°	VGP °N/°E
MN-1	Rhyolite	7	5	7/35	17/19.2	Magnetite	7	331/−8	38/9.9	52/264
MN-2	Rhyolite	6	2	331/31	–/–	Magnetite	6	341/−12	26/13.4	56/250
MN-3	Alkaline Trachyte	7	3	351/21	22/27	Magnetite	7	325/−4	32/11	48/273
MN-4	Carbonatite	7	5	358/9	28/14.8	Haematite	6	1/−7	22/14.5	64/213
MN-7	Alkaline Trachyte	7	6	7/44	20/15.4	Magnetite	7	337/−39	33/10.4	40.5/242
MN-8	Carbonatite	4	4	3/37	18/22	No stable characteristic remanent magnetization				
MN-9	Alkaline Trachyte	7	5	11/41	18/18.6	Magnetite	7	143/27	27/12	38.5/262
MN-10	Alk. Feld. syenite	6	2	9/63	–/–	Haematite	6	347/1	23/14	65/246
MN-11	Alk. Feld. syenite	5	3	334/26	19.5/28.7	Magnetite	5	311/−21	39.5/12	32/274
MN-13	Rhyolite	7	6	11/56	22/14.7	Magnetite	7	171/22	26.5/12	55/229
MN-14	Rhyolite	5	4	338/23	197/21	Magnetite	5	349/−17	40/12	57/234
MN-16	Alkaline Trachyte	7	2	6/17	22/56	Magnetite	7	326/−9	37/10	47.5/269
MN-17	Alkaline Trachyte	7	6	14/62	15/17.7	Magnetite	7	141/17	27.5/12	41/269
MN-18	Alkaline Trachyte	5	5	343/12	23.5/16	Haematite	3	344/−8	40.5/19.6	60/247
MN-20	Alk. Qz Syenite	6	4	352/54	20.6/21	Magnetite	6	332/−19	26/13.5	48/257
MN-21	Carbonatite	6	6	1/46	19/15.6	No stable characteristic remanent magnetization				
MN-23	Alk. Qz. Syenite	7	3	327/42	29/23	Magnetite	7	318/−26	30/11	35/266.5
MN-24	Alk. Qz. Syenite	5	2	349/44	–/–	Haematite	4	353/4	40/14.7	69/233
MN-25	Alk. Qz. Syenite	7	5	359/11	35/13	Magnetite	7	326/−27	43/9.3	40.5/259
MN-26	Alk. Feld. Syenite	7	2	1/52	–/–	Magnetite	7	149/10	36/10	49/266
MN-27	Rhyolite	7	5	21/46	23/16	Magnetite	7	161/22	27/12	52/245
MN-29	Alk. Feld. syenite	6	4	10/55	32/16.5	Magnetite	5	323/−17	34/13	43/268
		22/138	22/89	357/39	15.1/8.1	Magnetite mean	16/104	330/−19	35.3/6.3	47/259 Dp = 3.4°/Dm = 6.6°
						Haematitemean	4/19	351/−2.5	72.4/10.9	65/235.5 K = 112.6 α95 = 8.7°

remanence carrier in higher majority of the samples, while haematite (the curves with squares) was the main contributor in fewer samples (as MN-4-5 and Mn-10-3). Also, some samples showed the competitive coexistence of haematite with the magnetite (as Mn-5-3 and MN-19-6). As the higher curie-temperature haematite could obscure the magnetite primary remanence and prohibits its isolation as a discrete magnetic direction during thermal demagnetization, the studied sites were initially categorized into magnetite-dominated and haematite-dominated, before the paleomagnetic study. Each of them was, then, separately thermally demagnetized to reveal the natural remanence direction of the magnetite and haematite, to compare between them and test their genetic relation. However, few sites showing equal coexistence of magnetite with haematite [as MN-5-3 and MN-19-6] were eliminated from the paleomagnetic analysis to avoid the possible complex concurrent decay (yielding curved trajectories) of their magnetite remanence in the presence of haematite, if this haematite was developed by secondary processes long after the formation of rocks, although this is not proven in the present study.

In the subsequent IRM scheme, sites dominated by either magnetite or haematite were, imparted an IRM of 800 mT, then, progressively thermally demagnetized (Fig. 2), to monitor the thermal decay of their acquired IRM (the dashed curves with diamonds). The inspection of Fig. 2 elucidates the goethite contributions in both the magnetite- or haematite-dominated sites. This step shows that the haematite-dominated sites [such as MN-4-5, MN-10-3 (Fig. 2)], have appreciable goethite as magnetic carriers, reflected by the sharp major decay upon thermal demagnetization at 150 °C. On the other hand, most magnetite-dominated sites, have no or little contribution from goethite on their IRM [like samples MN-3-5, MN-9-2, MN-26-5, MN-29-4 and many others (Fig. 2)].

5. Natural remanence thermal demagnetization

Twin specimens from the same core were selected from each of the magnetite-dominated and haematite-dominated sites for both progressive alternating field [AF] and thermal demagnetization. The visual inspection of the decay trajectories in the orthogonal projections (Zijderveld, 1967) of these samples revealed the capability of thermal demagnetization to resolve

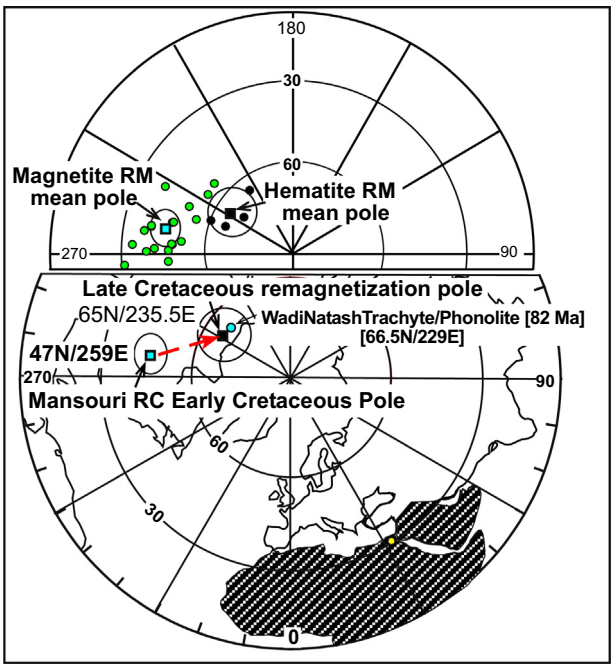

Fig. 5 The virtual geomagnetic poles [VGPs] of the site-means together with the mean paleomagnetic pole of both the haematite remanence (middle–Late Cretaceous secondary chemical remagnetization) and the magnetite ChRM remanence representing the Lower Cretaceous [132 Ma] paleomagnetic pole of Mansouri ring complex.

the remanent magnetization in all samples. On the other hand, AF demagnetization has failed to demagnetize the haematite-dominated samples and recover their remanence.

Accordingly, all samples were progressively thermally demagnetized up to fifteen steps, using 50 °C increment till 200 °C then becoming 100 °C till 450 °C then returning to 25 °C increment till complete demagnetization. Based on their magnetic remanence carriers, samples exhibited different demagnetization behaviors.

1. The magnetite samples (Fig. 3A), were characterized by the early decay of a soft northward normal medium-inclination magnetic component parallel to the present-day magnetic field [PDF] in the study area. This component was isolated and considered as PDF overprint residing in goethite. Subsequently, the magnetic trajectories change their directions to a steady NW-SE direction with shallow bipolar trajectories till complete demagnetization at about 585 °C (Fig. 3A). This NW–SE stable anchored magnetic component was overwhelming in most samples. It was, therefore, considered as the characteristic remanent magnetization of the Mansouri ring complex representing the Early Cretaceous magnetic field during the emplacement of the complex.
2. On the other hand, the haematite samples (Fig. 3B), after the decay of the soft PDF overprint at < 150 °C, their trajectories changed to a very shallow northward direction swinging up and down about zero inclination up to the complete decay at 680 °C. As this magnetic remanent is restricted to and residing in haematite samples, it is considered as a Late Cretaceous secondary chemical remagnetization, related to the eruption of Wadi Natash alkaline volcanic field, which, apparently, affected large areas of the Southeastern Desert after the intrusion of Mansouri Complex in the Early Cretaceous.

The isolated magnetite-residence ChRM mean magnetic direction passed a positive reversal test (McFadden and Lowes, 1981) at the 95% confidence level. The normal polarized sites [N = 11, Dec.,/Inc. = 329°/−18.3°, resultant vector (R) = 10.69, K = 32.69], and the reverse sites [N = 5, Dec.,/Inc., 152.9°/20°, R = 4.89, K = 36.05] share a common mean at the 95% confidence level and thus point that the antipodal means of this component are clean from secondary overprints.

6. Paleomagnetic results interpretation

The visual inspection of the demagnetization trajectories in the orthogonal projection (Zijderveld, 1967), revealed the bi-vectorial decay of most samples. After the early disintegration of the soft PDF component (< 150 °C) residing in goethite, which was isolated in eighty-nine samples (Fig. 4), trajectories change their directions and either one of two stable anchored components decays: a magnetite component (400–585 °C) or a haematite one > 585 °C.

The high-blocking temperature magnetite component, which was presented in antipodal polarities with distinct NW–SE declination and shallow to medium inclination, was present in one-hundred and four samples (Fig. 4, upper part).

Table 2 Euler pole rotation parameters used to rotate the paleomagnetic poles of the main tectonic units to NE Africa coordinates. Latitudes are reckoned (+) North, and (−) South, longitudes are (+) East, and (−) West, rotation angles are (+) counterclockwise and (−) clockwise.

Tectonic units rotated	Euler pole rotation parameters			References
	Latitude [°]	Longitude [°]	Angle [°]	
Greenland versus North American Craton	67.5	−118.48	−13.78	Roest and Srivastava (1989)
Stable Europe versus N. American Craton	68.99	154.75	−23.05	Srivastava and Roest (1989)
N. American Craton versus NW Africa	66.14	−18.72	58.03	Roest et al. (1992)
Amazonia versus S. Africa	50.0	327.5	55.1	Torsvik et al. (2009)
Parana versus S. Africa	47.5	326.7	56	Torsvik et al. (2009)
NW Africa versus S. Africa	33.6	26.0	2.3	Torsvik et al. (2012)
S. Africa versus NE Africa	40.5	−61.4	0.7	Torsvik et al. (2012)

Table 3A Early Cretaceous paleomagnetic North poles of the North American Craton rotated to NE Africa coordinates using Euler pole rotations parameters in Table 2. $K/\alpha 95$ denotes the precision parameter and the semi-angle of the 95% cone of confidence about the pole (Fisher, 1953).

Rock-unit	Age	$K/\alpha 95$ [°]	North pole (°N/°E)	NE Africa (°N/°E)	References
Lamprophyre dykes, Notre Dame Bay, NFL, Canada	122 ± 10	78/4.4	74/201	51/265	Prasad (1981)
Monteregian Hills intrusives, Quebec, Canada	122 ± 5	49/2.4	72/191	50/263.5	Foster and Symons (1979)
White Mountain Ig. Complex, NH, Ca	123 ± 4	275/3.3	71/187.5	50/261.5	Van Fossen and Kent (1992)
Southern Maine intrusives, USA	123 ± 3	86/2.4	72/199	49.5/266	McEnroe (1996)
Mont Megantic Intr, Quebec, Ca	130 ± 10	28/4.1	75/181	54/261	Seguin and St-Hilaire (1985)
Mt. Ascutney gab. VT, USA	133 ± 7	499/11	64.5/187	42.5/258.5	Opdyke and Wensink (1966)
Lamprophyre dykes, Notre Dame Bay, NFL, Canada	133 ± 7	180/3.6	67/212	43/273	Lapointe (1979)
Ithaca kimberlites, NY, USA	142 ± 5	550/2.6	58/203	34.5/263	Van Fossen and Kent (1993)
Mean of the North American Craton [N = 8 poles]	Early Cretaceous	338/3		47.2/264	

Table 3B Early Cretaceous paleomagnetic North poles of Stable Europe and Greenland rotated to NE Africa coordinates using Euler pole rotations parameters (Table 2). N.A.C. denotes poles in the North American Craton coordinates.

Rock-unit	Age	$K/\alpha 95$ [°]	North pole (°N/°E)	NE Africa (°N/°E)	References
Vectis Fm., Isle of Wight, Eng.	123 ± 5	148/21	61/188.5	37.5/250.5	Kerth and Hailwood (1988)
Berriasian limestone, France	140	16/2.9	74/183	48/260	Galbrun (1985)
Hinlopenstretet dolerites, Norway	144 ± 5	118/4	66/200	38/259	Halvorsen (1989)
Coast-parallel dike swarm, comb., Greenland	135	–/4.5	73.4/178	56/262.5	Torsvik et al. (2001)
Mean of Stable Europe and Greenland [N = 4 poles]	Early Cretaceous	71/11		45/257.5	

On the other hand, the highest-temperature haematite component, which had only normal polarity with swinging about the N direction and a very shallow equatorial inclination was only isolated in nineteen samples (Fig. 4, lower part).

In each sample, the best-fit line of at least three successive demagnetization steps of each of the visually isolated well-defined components was calculated using the principal component analysis [PCA] technique (Kirschvink, 1980) and plotted in Fig. 4. Subsequently, the site-mean directions of each of the aforementioned magnetic components were calculated with the associated statistical parameter; the precision parameter (K) and the semi-angle of the cone of 95 confidence ($\alpha 95$) (Fisher, 1953) (Fig. 4, Table 1). Then, the overall mean direction of each component was calculated with its statistical parameters (Fig. 4, Table 1).

The virtual geomagnetic poles [VGPs] of the two anchored components were determined for each site followed by the overall paleomagnetic pole of each of the magnetite and the haematite magnetic components with its statistical parameters (Fig. 5, Table 1)

The obvious parallelism of the soft normal goethite-residence component (359°/39°) with the present-day field [PDF] in the study area, supported its previous consideration as a recent PDF overprint in the samples. However, the clear resemblance of the haematite pole [65°N/235.5°E] (Fig. 5, Table 1) with the Late Cretaceous pole of the Trachyte/phonolite dykes (86–78 Ma) [66.5°N/229°E], of the volcanic field of Wadi Natash in the Southeastern Desert of Egypt (Lotfy, 2011), refers the haematite remanence to a Late Cretaceous chemical remagnetization inherited by secondary haematite.

On the other hand, the overwhelming occurrence of the magnetite remanence direction in 16 sites/104 samples points to it as the characteristic remanent magnetization [ChRM] of Mansouri ring complex. Therefore, the corresponding paleomagnetic pole [47°N/259°E] (Fig. 5, Table 1) can be, trustfully considered as representing the paleomagnetic field during the formation of the ring complex in the Lower Cretaceous (132 Ma).

7. Discussion and Euler pole rotations

In order to constrain the reliability of Mansouri complex Early Cretaceous paleomagnetic poles, it was compared with both:

Table 3C Early Cretaceous paleomagnetic North poles of South America (Craton and Parana) rotated to NE Africa coordinates using Euler pole rotations parameters (Table 2).

Rock-unit	Age	$K/\alpha 95$ [°]	North pole (°N/°E)	NE Africa (°N/°E)	References
Vulcanitas Cerro Colorado F, Cordoba, Arg	121 ± 6	42/10	81/194	44/253.5	Valencio (1972)
Cerro Barcino and Los Adobes, Patagonia. Arg.	122 ± 10	/2.9	87/339	54/262.5	Geuna et al. (2000)
Florianopolis dyke swarm (Santa Catarina Isl.), Br.	123 ± 5	46/2.6	89/183	54/258.5	Raposo et al. (1998)
El Salto-Almafuerte lavas, Cordoba, Arg.	124 ± 5	43/6	72/205	34.5/254	Mendia (1978)
Central Parana alk. Province Paraguay	128.5 ± 2	/3.1	85.4/242	48.5/261	Ernesto et al. (1996)
Sierra de Los Condores gp, Cordoba, Arg.	Ca 130	39/2.8	86/256	50/262	Geuna and Vizan (1998)
Arapey Fm, N. Uruguay	130	/4.2	85/276	50/265	Solano et al. (2010)
Northern Parana Magmatic Province	130 ± 2	–/2.4	83/251	46.5/264	Ernesto et al. (1999)
Serra Geral F., young Gp., Br, Urg	131 ± 4	–/7.7	82/218	47/260	Ernesto et al. (1990)
Ponta Grossa dykes, Br.	131 ± 4	43/2	82/210	47/258	Raposo and Ernesto (1995)
Central Parana Basin	132	/2.3	84/244	47/262.5	Raposo and Ernesto (1995)
Central Parana Magmatic Prov., B	132.5	/2.6	86/378	56.5/260.5	Alva-Valdivia et al. (2003)
Mean S. America Early Cret.	132.5 ± 3	/2	85/256.5	51/244.5	Somoza and Zaffarana (2008)
Southern Parana Basin	133	/1.5	84/286	50/267	Raposo and Ernesto (1995)
Alto Fm, Paraguay	134	/4.3	86/179	49/255.5	Goguitchaichvili et al. (2012)
Alto Fm, Paraguay	134	/3.6	86/214	48.5/258	Goguitchaichvili et al. (2012)
Serra Geral Basalts, Br.	135 ± 4	40/3.7	84.5/295.5	53.5/268.5	Pacca and Hiodo (1976)
Serra Geral F., Br, Urg	135 ± 4	22/5.7	78/234	43.5/264.5	Creer (1962)
Serra Geral F., Br	135 ± 4	30/3	83.5/280.5	51.5/269	Bellioni et al. (1983)
Serra Geral F., Main Gp., Br, Urg.	135 ± 4	–/1.2	85/288	53/267	Ernesto et al. (1990)
Rio de Los Molinos dykes 2, Cordoba, Arg.,	139.5 ± 10	50/11	79/188	42.5/251	Linares and Valencio (1975)
Mean of South America [N = 21 poles	Early Cretaceous	186/2.3		48.8/261	

Table 3D Early Cretaceous paleomagnetic North poles of Africa rotated to NE Africa coordinates using Euler pole rotations parameters (Table 2).

Rock-unit	Age	$K/\alpha 95$ [°]	North pole (°N/°E)	NE Africa (°N/°E)	References
Kaoko lavas, Namibia	132 ± 10	53/3	48/266.6	47.5/266.6	Gidskehaug et al. (1975)
Cretaceous Kimberlites Group II, S. Africa	129 ± 16	–/9.7	47.6/270	47/270	Hargraves (1989)
Central Atlas Intrusions, South Morocco	143 ± 21	10/22	53/261.5	51.5/264	Hailwood and Mitchell (1971)
Ramon anticline basalts, Israel	Early Cret.	15/8.6	53/265	53/265	Helsley and Nur (1970)
Essexite Laccolith, Israel	Early Cret.	84/14	48/265.5	48/265.5	Freund and Tarling (1979)
Mean of Africa [N = 5 poles]	Early Cretaceous	693/2.9		49/266	

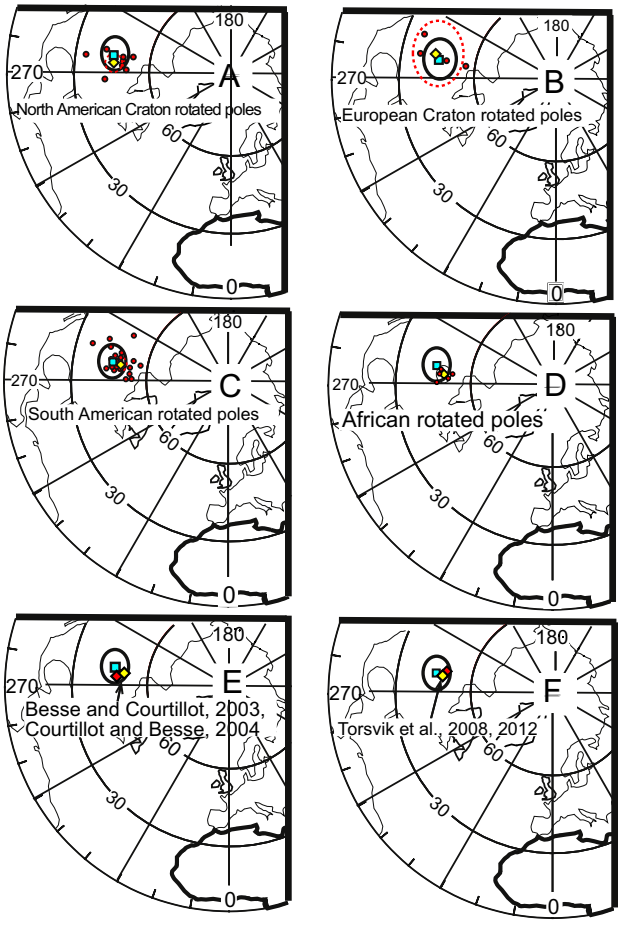

Fig. 6 A–D. Early Cretaceous paleomagnetic North poles of the main tectonic units rotated to NE Africa coordinates (Tables 3A–3D) and their respective mean poles and cones of 95% confidence [A95] (dash circles) compared to the Early Cretaceous pole of the present study with its cone of 95% confidence [A95] (Table 4). E and F. Early Cretaceous pole of the present study with its [A95] compared to the mean coeval poles from the recent global APWPs rotated to NE Africa coordinates (E, Besse and Courtillot, 2002, 2003; Courtillot and Besse, 2004, F, Torsvik et al., 2008, 2012).

1. The coeval Early Cretaceous poles of the main tectonic units namely; the North American Craton, Stable Europe, South America and Africa, rotated to NE Africa coordinates using the appropriate Euler pole rotation parameters (Tables 2 and 4). These poles were collected from the global databases (McElhinny and Lock, 1996; Pisarevsky, 2005; Van der Voo, 1993) and some recent global reconstructions (Torsvik et al., 2008, 2012).
2. The Early Cretaceous poles of some recent Global Apparent Polar Wander Paths [APWPs] such as Besse and Courtillot (2002, 2003), Courtillot and Besse (2004) and Torsvik et al. (2008, 2012) (Table 4).

As one of the best paleomagnetically studied continents, eight poles were selected from the North American Craton. These poles were, first, rotated to NW Africa using the rotation parameters of Roest et al. (1992) for M11 anomaly [133.1 Ma] (Table 2). These poles were, then, internally rotated from NW to NE African coordinates using Torsvik et al. (2012) parameters. The rotated poles (Table 3A) are well-clustered with their mean pole at 47.2°N/264°E [K = 338/$\alpha 95$ = 3°] (Tables 3A and 4). The rotated mean pole was along the same latitude of Mansouri poles but at slightly higher longitude with its cone of 95% confidence completely enclosed in that of Mansouri complex (Fig. 6A, Table 4).

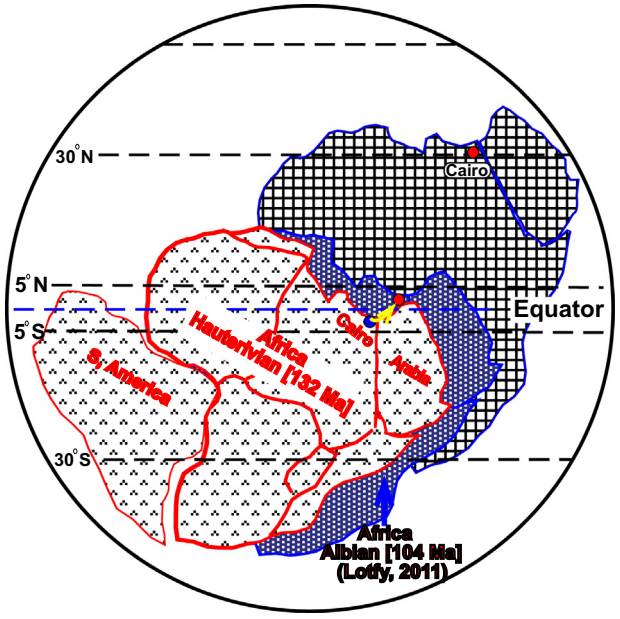

Fig. 7 Paleo-tectonic position of Africa within Gondwana in the Early Cretaceous [Hauterivian] showing NE Africa (Cairo) south the Equator but within the equatorial zone [±5° around the Equator]. Present-day position of Africa with Cairo at 30°N is presented for comparison.

Only three poles from Stable Europe and one from Greenland were collected and rotated to the North American Craton coordinates using the rotation parameters of Roest and Srivastava (1989) and Srivastava and Roest (1989) (Table 2), respectively. These poles were, then, rotated to NE Africa following the same sequence of the North America Craton poles. The rotated European poles (Table 3B) are slightly dispersed with their dispersion parameters being K = 71, $\alpha 95$ = 11° about a mean pole at 45°N/257.5°E (Tables 3B, 4). Despite the dispersion of the European poles, their mean pole fits well with Mansouri pole (Table 4), with the cone of 95% confidence of the later completely enclosed in the former (Fig. 6B).

From both Amazonia and Parana tectonic units in South America, twenty-one poles were rotated to South Africa coordinates (Torsvik et al., 2009), then internally rotated to NE Africa (Torsvik et al., 2012). The rotated poles fairly cluster around their mean pole at 48.8°N/261°E [K = 186/$\alpha 95$ = 2.3°] (Tables 3C and 4, Fig. 6C). The South America mean pole lies close to Mansouri pole (Table 4) and enclosed in its cone of confidence (Fig. 6C).

Due to their scarcity, only three poles were collected from Africa and added to two wide-age Early Cretaceous poles from Israel (Table 3D). These African poles are, then, internally rotated to NE Africa using the rotation parameters of Torsvik et al. (2012). Despite their limited number, the rotated poles are well-clustered about their mean at 49°N/266°E [K = 693/$\alpha 95$ = 2.9°] (Tables 3D and 4, Fig. 6D). The NE

Table 4 A. Early Cretaceous paleomagnetic North pole of the African Plate of the Mansouri ring complex. B. Mean Early Cretaceous poles rotated from the main tectonic units with the overall mean of the four continents rotated to NE Africa coordinates. C. Mean Early Cretaceous [140–120 Ma] mean poles from recently calculated Global Apparent Polar Wander Paths [APWP] rotated to NE Africa coordinates. [K/α95] denote the precision parameter and the semi-angle of the 95% cone of confidence around the mean pole. Cairo Ref. and Plat. denote the corresponding Early Cretaceous paleo-declination, paleo-inclination and paleo-latitude predicted at the reference location of Cairo, Egypt [30°N/31°E], from the cited poles.

A	Ring Complex	Age [Ma]	Sites	Pole (°N/°E) [NE Africa]	Dp°/Dm°	Cairo Ref. [Dec.°/Inc.°]	Plat. [°]
1	Mansouri R. C. [22.05°N/33.63°E]	132 ± 10 Ma [Rb/Sr]	16	47 N/259E	3.4/6.6	329.5/−3.4	−1.7
B	Tectonic unit	Age [Ma]	N	Mean pole (°N/°E) [NE Africa]	K/α95 [°]		
1	North American Craton	132 ± 10	8	47.2/264	338/3	327/1.5	.75
2	Stable Europe	132 ± 10	4	45/257.5	71/11	329/−7.8	−3.9
3	S. America (Amazonia and Parana)	132 ± 10	21	48.8/261	186/2.3	329.5/1	.5
4	Africa	132 ± 10	5	49.4/266	694/2.9	328/6	3
	Mean of four continents	132 ± 10	4	47.5/262	70.5/3.5	328.5/0	0
C	Global APWP	Age [Ma]	N	Mean pole (°N/°E) [NE Africa]	α95		
1	Global APWP Besse and Courtillot (2002, 2003) rotated to NE African coordinate	120	20	53.7/261	2.7	333/8	4
		130	14	49.7/262	2.9	330/3	1.5
		140	7	45.4/264.5	6.2	325.5/−1	−.5
2	Global APWP Courtillot and Besse (2004) rotated to NE African coordinate	120	26	53.5/260.6	2.0	333/8	4
		130	23	50.3/261.7	2.1	330.5/4	2
		140	13	49.1/265.2	5.7	328/5	2.5
3	Global APWP Torsvik et al. (2008) rotated to NE African coordinate	120	24	53.5/261.2	2.6	332.5/8	4
		130	18	50.3/260	2.9	331/2.5	1.2
		140	10	48.8/253	6.1	334/−5.5	−2.75
4	Global APWP Torsvik et al. (2012) rotated to NE African coordinate	120	28	53.3/261.2	2.6	332.5/8	4
		130	18	49/261	2.8	330/1.5	.75
		140	9	45.5/262	6	327/−3	−1.5

Table 5 Early Cretaceous paleomagnetic pole of the African Plate of the present study (upper part) compared to coeval poles of some Eastern Mediterranean tectonic blocks (lower part) with their predicted paleo-latitudes calculated at the reference location of Cairo (Egypt) [30°N/31°E].

	Age [Ma]	$K/\alpha 95$ [°]	North pole (°N/°E)	Predicted paleo-latitude at Cairo [°]	References
Mansouri ring complex	132 ± 10	35.3/6.3	47/259	−1.7	Present study
Eastern Mediterranean blocks					
Gorgo a Cerbara Section, N Umbr.	123 ± 5	14/3	19/296	5	Lowrie and Alvarez (1984)
Presale Section, N Umbria	122 ± 4	18/3	24/293	5.5	Lowrie and Alvarez (1984)
Frontale Section, N Umbria	124 ± 6	15/4	32/278	−1.3	Lowrie and Alvarez (1984)
Maiolica Ls., Umbria, Italy [comb.]	134 ± 15	70/15	25.5/289	3	Lowrie and Alvarez (1984)
Maiolica Fm., N. Umbian Arc	131 ± 16	57/5	32/282	1.5	Hirt and Lowrie (1988)
Maiolica Fm., S. Umbian Arc	131 ± 16	33/7	48/264	1.3	Hirt and Lowrie (1988)
Maiolica Fm., Giordano, N. Umbr.	142 ± 10	158/10	19/288	−1.2	Cirilli et al. (1984)
Maiolica Fm., Switz. and N. Italy	132 ± 8	33/12	57/247	2	Channell et al. (1993)
Maiolica Ls. Italy	129 ± 11	49/11	42/273	1.7	Channell et al. (1995)
Cismon Section, S. Alps, Italy	124 ± 4	12/2.3	44/257	−4.7	Channell et al. (2000)
Umbrian sed, Umbria, It	139 ± 15	291/3	30/281	−.5	Channell (1992)
Abruzzi sed.,1, Apennines, Italy	129 ± 17	44/14	59/247	3.7	Marton and D'Andrea (1992)
Cretaceous Ls, Transdanub., Hung.	139 ± 7	46/18	20/298	7.4	Marton and Marton (1983)
Theopetra area, Thessalia, Greece	130 ± 5	–/3	47/267	2	Surmont (1989)
Tithonian- Aptian sed, Adria	132 ± 20	67/9.4	47/275	6	Márton et al. (2008)
Umbria- Marche Section	130 ± 1.2	37/2.5	32/285	3.5	Satolli et al. (2007)

African mean pole lies at higher latitude and longitude with respect to Mansouri pole but its cone of confidence largely overlapping with that of the complex (Fig. 6D).

For the sake of comparison, the mean poles rotated from the North American Craton, Stable Europe, South America and Africa were used to calculate an overall mean Early Cretaceous pole for the four continents giving a unit weight to each continent (Table 4). The four continents means are well-clustered around both their overall mean at 47.5°N/262°E [$K = 705$, $\alpha 95 = 3.5°$] and Mansouri mean (47°N/259°E) (Table 4).

Two further comparisons of Mansouri Complex pole were made with the recent global APWPs rotated to NE Africa coordinates. The mean poles of 130 Ma of Besse and Courtillot (2002, 2003), Courtillot and Besse (2004) and Torsvik et al. (2008, 2012) (Table 4), are all very close to Mansouri pole (Fig. 6E and F).

8. Conclusion and Early Cretaceous paleo-tectonic position of NE Africa

The Early Cretaceous paleomagnetic pole of the Mansouri ring complex (132 ± 10 Ma), which lies at 47°N/259°E, generally fits well with the following synchronous poles:

1. Mean poles rotated to NE Africa from the four main continents: the North American Craton, Stable Europe, South America [Amazonia and Parana] as well as Africa.
2. Mean Early Cretaceous poles [130 Ma] rotated from the recent Global Apparent Polar Wander Paths [APWPs].

Therefore, the Mansouri paleomagnetic pole can, reliably, be considered as representing the paleomagnetic field during the emplacement of the Mansouri ring complex in the Early Cretaceous [Hauterivian]. This pole places Africa in a paleo-tectonic position far from its present-day position:

1. In terms of paleo-azimuth, Africa was about 30° clockwise with a northeastwards azimuth with respect to the present-axial N–S direction.
2. In terms of paleo-latitude, NE Africa was equatorial with Cairo (now at 30°N) was just south of the Equator at 1.5°S paleo-latitude. This means that Africa was about 31° southwards from its present-day latitudes (Fig. 7).

In order to further constrain the equatorial paleo-tectonic position of NE Africa, a number of Early Cretaceous paleomagnetic poles of some Eastern Mediterranean blocks were collected from the paleomagnetic databases (McElhinny and Lock, 1996; Pisarevsky, 2005; Van der Voo, 1993). Their computed Early Cretaceous directions and paleo-latitudes at the reference location of Cairo (30°N/31°E) were calculated (Table 5). The inspection of the computed paleo-latitudes of Umbria, Italy, Adria, Apennines and Greece (Table 5) reflects their unequivocal Early Cretaceous equatorial paleo-latitudes probably just north of NE Africa.

Comparing the Mansouri Hauterivian pole [47°N/259°E] to the Albian paleomagnetic pole during the emplacement of the Wadi Natash volcanic field alkaline basalts [107 ± 4 Ma], which was at [55°N/250°E], the African Plate seems to have rotated counter-clockwise about 10° with Northeast Africa moving slightly northwards [Cairo was moving from 1.5°S to 1.5°N] within the equatorial zone, during the Early Cretaceous (Fig. 7).

Acknowledgments

This research would not have been possible without the kind support and help of Prof. Dr. Hatem H. Odah, President of the National Research Institute of Astronomy and Geophysics [NRIAG] and Prof. Dr. Esmat Abd El-All, Chairman of the Department of Geomagnetism and Geoelectricity. The author is deeply indebted to Prof. E. Abd El-All and all her colleagues

and staff members of the Geomagnetism Laboratory, for offering their Paleomagnetic Laboratory for this research and their strenuous efforts during its progress. This research was supported by the official research funds of Minia University, Minia, Egypt, given to the Faculty members at the Faculty of Science.

Sincere thanks are all due to the reviewers of this papers, whose critical and insightful comments and suggestions greatly improved the manuscript.

References

Alva-Valdivia, L.M., Goguitchaichvili, A., Urrutia-Fucugauchi, J., Riisager, J., Riisager, P., Ferreira-Lopes, O., 2003. Paleomagnetic poles and paleosecular variation of basalts from Parana Magmatic Province, Brazil: geomagnetic and geodynamic implications. Phys. Earth Planet. Interiors 138, 183–196.

Bellioni, G., Brotzu, P., Conin-Chiaramonti, P., Ernesto, M., Melfi, A.J., Pacca, I.G., Piccirilla, E.M., Stolfa, D., 1983. Petrological and paleomagnetic data on the Plateau basalt to rhyolite sequences of the southern Parana Basin, (Brazil). Anais. Acad. Brazil Cienc. 55, 355–383.

Besse, J., Courtillot, V., 2002. Apparent and true polar wander and the geometry of the geomagnetic field over the last 200 Myr. J. Geophys. Res. 107 (B11), 2300. http://dx.doi.org/10.1029/2000JB000050.

Besse, J., Courtillot, V., 2003. Correction to "Apparent and true polar wander and the geometry of the geomagnetic field over the last 200 Myr". J. Geophys. Res. 108 (B10), 2469. http://dx.doi.org/10.1029/2003JB002684.

Channell, J.E.T., 1992. Paleomagnetic data from Umbria (Italy): implications for the rotation of Adria and Mesozoic apparent polar wander paths. Tectonophysics 216, 365–378.

Channell, J.E.T., Cecca, F., Erba, E., 1995. Correlations of Hauterivian and Barremian (Early Cretaceous) stage boundaries to polarity chrons. Earth Planet. Sci. Lett. 134, 125–140.

Channell, J.E.T., Erba, E., Lini, A., 1993. Magnetostratigraphy calibration of the Late Valanginian carbon isotope event in pelagic limestones from northern Italy and Switzerland. Earth Planet. Sci. Lett. 118, 145–166.

Channell, J.E.T., Erba, E., Muttoni, G., Tremolada, F., 2000. Early Cretaceous magnetic stratigraphy in the APTICORE drill core and adjacent outcrop at Cismo (Southern Alps, Italy), and correlation to the proposed Barremian-Aptian boundary stratotype. Geol. Soc. Am. Bull. 112, 1430–1443.

Cirilli, S., Marton, P., Vigli, L., 1984. Implications of a combined biostratigraphic and paleomagnetic study of the Umbrian Maiolica Formation. Earth Planet. Sci. Lett. 69, 203–214.

Cohen, K.M., Finney, S.C., Gibbard, P.L., Fan, J.-X., 2013. The ICS international chronostratigraphic chart. Episodes 36, 199–204.

Courtillot, V., Besse, J., 2004. A long-term octupolar component in the geomagnetic field? (0–200 million years B.P.). In: Timescales of the Paleomagnetic Field, Geophysical Monograph Series 145, America Geophysical Union. doi: http://dx.doi.org/10.1029/145GM05.

Creer, K.M., 1962. Palaeomagnetism of the Serra Geral Formation. Geophys. J. Roy. Astron. Soc. 7, 1–22.

Daly, M.C., Chorowicz, J., Fairhead, J.D., 1989. Rift basin evolution in Africa: the influence of reactivated steep basement shear zones. In: Cooper, M.A., Williams, G.D. (Eds.), . In: Inversion Tectonics, 44. Geological Society [London] Special Publication, pp. 309–334.

El-Nisr, S.A., Saleh, G.M., 2001. Geochemistry and petrogenesis of the late jurassic-early cretaceous Mansouri ring complex, Southeastern desert, Egypt. J. Afr. Earth Sci. 32 (1), 87–102.

El Ramly, M.F., Budanov, V.I., Hussein, A.A., Dereniuk, N.E., 1970. Ring complexes in the south eastern desert of Egypt. In: Moharram, et al. (Eds.), Studies on Some Mineral Deposits of Egypt. Geol. Surv. Egypt, pp. 181–194

El-Ramly, M.F., Budanov, V.I., Hussein, A.A., 1971. The Alkaline rings of south eastern Egypt. Geol. Surv. Egypt 53, 1–111.

El Ramly, M.F., Hussein, A.A., 1982. The alkaline ring complexes of Egypt. Geol. Surv. Egypt Pap. 63, 16p.

El-Ramly, M.F., Hussein, A.A., 1985. The ring complexes of the eastern desert of Egypt. J. Afr. Earth Sci. 3, 77–82.

El-Reedy, M.W.M., 1979. Geochronological and geochemical studies on the alkalic rocks in the south Eastern Desert of Egypt. Ph.D., thesis, Faculty of Science, Cairo University.

Ernesto, M., Comin-Chiaramonti, P., Gomes, C.B., Castillo, A.M., Velazquez, J.C., 1996, Palaeomagnetic data from the Central Alkaline Province, Eastern Paraguay. In: Gomes, C.B., Comin-Chiaramonti, P. (Eds.), Alkaline magmatism in Central-Eastern Paraguay: Sao Paulo, EDUSP/FAPESP, pp. 85–102.

Ernesto, M., Pacca, I.G., Hiodo, F.Y., Nardy, A.J.R., 1990. Palaeomagnetism of the Mesozoic Serra Geral Formation, southern Brazil. Phys. Earth Planet. Interiors 64, 153–175.

Ernesto, M., Raposo, M.I.B., Marques, L., Renne, P., Diogo, L., Min, M., 1999. Paleomagnetism, geochemistry and 40Ar/39Ar dating of the Northeastern Parana Magmatic Province. J. Geodyn. 28, 321–340.

Fisher, R.A., 1953. Dispersion on a sphere. Proc. Roy. Soc. Lond. A217, 295–305.

Foster, J., Symons, D.T.A., 1979. Defining a paleomagnetic polarity pattern in the Monteregian intrusives. Can. J. Earth Sci. 16, 1716–1725.

Freund, R., Tarling, D.H., 1979. Preliminary paleomagnetic results from Israel and inferences for a microplate structure in the Lebanon. Tectonophysics 60, 189–205.

Galbrun, B., 1985. Magnetostratigraphy of the Berriasian stratotype section (Berrias, France). Earth Planet. Sci. Lett. 74, 130–136.

Garson, M.S., Krs, M., 1976. Geophysical and geophysical evidence of the relationship of Red Sea transverse tectonics to ancient features. Bull Geol. Soc. Am. 87, 169–181.

Garfunkel, Z., 1992. Darfur-Levant array of volcanics – a 140-Ma-long record of a hot spot beneath the African-Arabian continent, and its bearing on Africa's absolute motion. Israel J. Earth Sci. 40, 135–150.

Geuna, S.E., Somoza, R., Vizan, H., Figari, E.G., Rinaldi, C.A., 2000. Paleomagnetism of Jurassic and Cretaceous rocks in Central Patagonia: a key to constrain the timing of rotations during the breakup of southwestern Gondwana? Earth Planet. Sci. Lett. 181, 145–160.

Geuna, S.E., Vizan, H., 1998. New Early Cretaceous palaeomagnetic pole from Cordoba Province (Argentina): revision of previous studies and implications for the South American database. Geophys. J. Int. 135, 1085–1100.

Gidskehaug, A., Creer, K.M., Mitchell, J.G., 1975. Palaeomagnetism and K-Ar ages of the South West African Basalts and their bearing on the time of initial rifting of the South Atlantic Ocean. Gephys. J. Roy. Astron. Soc. 42, 1–20.

Goguitchaichvili, A., Solano, M., Camps, P., Sánchez Bettucci, L., Mena, M., Trindade, R., Reyes, B.A., Morales, J., Locra, H.L., 2012. The earth's magnetic field prior to the Cretaceous normal Superchron: new paleomagnetic results from Alto Paraguay Formation. Int. Geol. Rev. ifirst, 1–13.

Gradstein, F., Ogg, J., Schmitz, M., Ogg, G., 2012. The Geologic Time Scale 2012, first ed. Elsevier, Boston, USA. http://dx.doi.org/10.1016/B978-0-444-59425-9.00004-4.

Guiraud, R., Maurin, J.C., 1991. Le rifting in Afrique au Crétacé Inférieur: synthése structurale, mise en évidence de deux eétapes dans la genése des bassins, relations avec les ouvertures océanique péri-afriquaines. Bull. Soc. Géol. France 162, 811–823.

Guiraud, R., Maurin, J.C., 1992. Early Cretaceous rifts of western and central Africa: an overview. Tectonophysics 213, 153–168.

Hailwood, E.A., Mitchell, J.G., 1971. Palaeomagnetism and radiometric dating results from Jurassic intrusions in South Morocco. Geophys. J. Roy. Astron. Soc. 20, 28–34.
Halvorsen, E., 1989. A paleomagnetic pole position of Late Jurassic/Early Cretaceous dolerites from Hinlopenstretet, Svalbard, and its tectonic implications. Earth Planet. Sci. Lett. 94, 398–408.
Hargraves, R.B., 1989. Paleomagnetism of Mesozoic kimberlites in Southern Africa and the Cretaceous apparent polar wander curve for Africa. J. Geophys. Res. 94, 1851–1866.
Hashad, A.M., El-Reedy, M.W.M., 1979. Geochronology of the anorogenic alkalic rocks, South Eastern Desert, Egypt. Ann. Geol. Surv. Egypt IX, 81–101.
Heller, F., 1978. Rock magnetic studies of upper Jurassic limestones from southern Germany. J. Geophys. 44, 525–543.
Helsley, C.E., Nur, A., 1970. The paleomagnetism of Cretaceous rocks from Israel. Earth Planet. Sci. Lett. 8, 403–410.
Hirt, A.M., Lowrie, W., 1988. Paleomagnetism of the Umbrian-Marches orogenic belt. Tectonophysics 146, 91–103.
Janssen, M.E., Stephenson, R.A., Cloetingh, S., 1995. Temporal and spatial correlations between changes in plate motions and the evolution of rifted basins in Africa. Geol. Soc. Am. Bull. 107, 1317–1332.
Kerth, M., Hailwood, E.A., 1988. Magnetostratigraphy of the Lower Cretaceous Vectics Formation (Wealden Group) on the Isle of Wight, southern England. J. Geol. Soc. Lond. 14, 351–360.
Kirschvink, J.L., 1980. The least squares line and plane and the analysis of paleomagnetic data. Geophys. J. Roy. Astron. Soc. 62, 699–718.
Klemenic, P.M., 1987. Variable intra-plate igneous activity in central and north-east Sudan. J. Afr. Earth Sci. 6 (4), 465–474.
Klitgord, K,D., Schouten, H., 1986. Plate kinematics of the central Atlantic. In: Vogt, P.R., Tucholke, B.E. (Eds.), The western North Atlantic region, Geology of North America, v. M, pp. 351–378.
Lang, B., Hebeda, E.H., Priem, H.N.A., Steinitz, G., Verdurmen, E.A.T., 1988. K-Ar and Rb-Sr ages of Early Cretaceous magmatic rocks from Makhtesh Ramon, Southern Israel. Israel J. Earth Sci. 37 (2–3), 65–72.
Lang, B., Steinitz, G., 1989. K-Ar dating of Mesozoic magmatic rocks in Israel: a review. Israel J. Earth Sci., 38–103
Lapointe, P.L., 1979. Paleomagnetism of the Notre Dame Bay Lamprophyre dikes, Newfoundland, and the opening of the North Atlantic Ocean. Can. J. Earth Sci. 16, 866–976.
Linares, E., Valencio, D.A., 1975. Paleomagnetism and K/Ar ages of some trachybasaltic dykes from Rio de Los Molinos, Province of Cordoba, Republic of Argentina. J. Geophys. Res. 80, 3315–3321.
Lotfy, H.I., 2011. Active concomitant counterclockwise rotation and northwards translation of Africa during the Mid-Late Cretaceous: a paleomagnetic study on the Wadi Natash alkaline volcanic province (104–84 Ma), South Eastern Desert, Egypt. Palaeogeogr. Palaeoclim. Palaeoecol. 310, 176–190.
Lowrie, W., Alvarez, W., 1984. Lower Cretaceous magnetic stratigraphy in Umbria pelagic limestone sections. Earth Planet. Sci. Lett. 71, 315–328.
Márton, E., Ćosović, V., Moro, A., Zvocalk, S., 2008. The motion of Adria during Late Jurassic and Cretaceous: new paleomagnetic results from stable Istria. Tectonophysics 454, 44–53.
Márton, P., D'andrea, M., 1992. Palaeomagnetically inferred tectonic rotations of the Abruzzi and northwestern Umbria. Tectonophysics 202, 43–53.
Márton, E., Márton, P., 1983. A refined polar wander curve for the Transdanubian Central Mountains and its bearing on the Mediterranean tectonic history. Tectonophysics 98, 43–57.
Maurin, J.C., Guiraud, R., 1993. Basement control in the development of the Early Cretaceous West and Central African rift system. Tectonophysics 228, 81–96.
McElhinny, M.W., Lock, J., 1996. IAGA paleomagnetic databases with access. Surv. Geophys. 17 (5), 575–591, Doi:19.1038/2161276a0.
McEnroe, S.A., 1996. A Barremian-Aptian (Early Cretaceous) North American paleomagnetic reference pole. J. Geophys. Res. 101, 15819–15835.
McFadden, P.L., Lowes, F.J., 1981. The discrimination of mean directions drawn from Fisher distributions. Geophys. J. Roy. Astron. Soc. 67, 19–33.
Mendia, J.E., 1978. Palaeomagnetism of alkaline lava flows from El Salto-Almafuerte, Cordoba Province, Argentina. Geophys. J. Roy. Astron. Soc. 54, 539–546.
Meneisy, M.Y., 1990. Vulcanicity. In: Said, R. (Ed.), The Geology of Egypt. Balkema, Rotterdam, pp. 157–172.
Milner, S.C., Le Roex, A.P., O'Connor, J.M., 1995. Age of Mesozoic igneous rocks in north-western Namibia, and their relation to continental breakup. J. Geol. Soc. Lond. 152, 97–104.
Opdyke, N.D., Wensink, H., 1966. Paleomagnetism of rocks from the white Mountain Plutonic Volcanic series in New Hampshire and Vermont. J. Geophys. Res. 71, 3045–3051.
Pacca, I.G., Hiodo, F.Y., 1976. Paleomagnetic analysis of Mesozoic Serra Geral basaltic lava flows in southern Brazil. Ann. Acad. Brasil Cienc. 48, 207–216.
Pisarevsky, S.A., 2005. New edition of the global paleomagnetic database. EOS 86 (17), 170.
Prasad, J.N., 1981. Paleomagnetism of the Mesozoic Lamprophyre dykes in north-central Newfoundland. M.Sc. Thesis, Memorial University, Newfoundland, Canada.
Rabinowitz, P.D., Labrecque, J., 1979. The Mesozoic South Atlantic ocean and the evolution of its continental margin. J. Geophys. Res. 84, 5973–6003.
Raposo, M.I.B., Ernesto, M., 1995. An Early Cretaceous paleomagnetic pole from Ponta Grossa dikes (Brazil): implications for the South American Mesozoic apparent polar wander path. J. Geophys. Res. 100 (B10), 20095–20109.
Raposo, M.I.B., Ernesto, M., Renne, P.R., 1998. Paleomagnetism and 40Ar/39Ar dating of Early Cretaceous Florianopolis dike swarm (Santa Catarina Island), Southern Brazil. Phys. Earth Planet. Interiors 108, 275–290.
Roest, W.R., Danobeitia, J.J., Verhoef, J., Collette, B.J., 1992. Magnetic anomalies in the Canary Basin and the Mesozoic evolution of the central North Atlantic. Mar. Geophys. Res. 14, 1–24. http://dx.doi.org/10.1007/BF01674063.
Roest, W.R., Srivastava, S.P., 1989. Sea-floor spreading in the Labrador sea: a new reconstruction. Geology 17, 1000–1003. http://dx.doi.org/10.1130/0091-76B(1989) 017 < 1000:SFSITL > 2.5.CO;2.
Satolli, S., Besse, J., Speranza, F., Calamita, F., 2007. The 125–150 Ma high-resolution Apparent Polar Wander Path for Adria from magnetostratigraphic sections in Umbria–Marche (Northern Apennines, Italy): timing and duration of the global Jurassic-Cretaceous hairpin turn. Earth Planet. Sci. Lett. 257, 329–342.
Savostin, L.A., Sibuet, J.-C., Zonenshain, L.P., Le Pichon, X., Roulet, M.-J., 1986. Kinematic evolution of the Tethys belt from the Atlantic Ocean to the Pamirs since the Triassic. Tectonophysics 123, 1–35.
Seguin, M.K., St-Hilaire, B., 1985. Magnetochronologie des formations rocheuse du Mont Megantic et des environs, Quebec meridional. Can. J. Earth Sci. 22, 487–497.
Semtner, A.-K., 1993. Uplift kinematics of Jebel Dirurba sedimentary complex, Red Sea Hills, Sudan. In: Thorweibe, U., Schandelmeier, H. (Eds.), Geoscientific Research in Northeast Africa. Balkema, Rotterdam, pp. 255–258.
Serencsits, C.M., El-Ramly, M.F., Faul, H., Foland, K.A., Hussein, A.A., 1979. Alkaline ring complexes in Egypt: their age and relationship to tectonic development of the Red Sea. Ann. Geol. Surv. Egypt 9, 102–116.
Serencsits, C.M., Faul, H., Foland, K.A., El-Ramly, M.F., Hussein, A.A., Lutz, T.M., 1981. Alkaline ring complexes in Egypt: their ages and relationship in time. J. Geophys. Res. 86, 3009–3013.

Solano, M., Goguitchaichvili, A., Sánchez Bettucci, L., Ruiz, R., Calvo-Rathert, M., Ruiz-Martinez, V., Soto, R., Alva-Valdivia, L., 2010. Paleomagnetism of early cretaceous arapey formation (Northern Uruguay). Stud. Geophys. Geodaet. 54 (4), 533–546.

Somoza, R., Zaffarana, C., 2008. Mid-Cretaceous polar standstill of South America, motion of the Atlantic hotspots and the birth of the Andean cordillera. Earth Planet. Sci. Lett. 271, 267–277.

Srivastava, S.P., Roest, W.R., 1989. Seafloor spreading history II–IV, in East Coast Basin Atlas Series: Labrador Sea. Bell, J.S. (Ed.), Map, sheets L17-2- L17-6, Atl. Geosci. Cent., Geol. Surv. Can., Dartmouth, N.S.

Surmont, J., 1989. Paléomagnétisme dans les Hellénides internes: analyse des aimantations superposées par la méthod des cercles de réaimantation. Can. J. Earth Sci. 26, 2479–2494.

Torsvik, H.T., Muller, R.D., Van der Voo, R., Steingerger, B., Gaina, C., 2008. Global plate motion frames: toward a unified model. Rev. Geophys. 46, RG3004/2008, 1–44.

Torsvik, T.H., Rousse, S., Labails, C., Smerthurst, M., 2009. A new scenario for the opening of the South Atlantic Ocean and the dissection of an Aptian Salt Basin. Geophys. J. Int. 183 (1), 29–34.

Torsvik, T.H., Van der Voo, R., Meert, J.G., Mosar, J., Walderhaug, H.J., 2001. Reconstructions of the continents around the North Atlantic at about the 60th parallel. Earth Planet. Sci. Lett. 187, 55–69. http://dx.doi.org/10.1016/S0012-821X(01)00284-9.

Torsvik, T.H., Van der Voo, R., Preeden, U., Mac Niocaill, C., Steinberger, B., Doubrovine, P., van Hinsbergen, D.J.J., Domeier, M., Gaina, C., Tohver, E., Meert, J.G., McCausland, P.J.A., Cocks, L.R.M., 2012. Phanerozoic polar wander, paleogeography and dynamics. Earth-Sci. Rev. 114, 325–368.

Valencio, D.A., 1972. Palaeomagnetism of the Lower Cretaceous Vulcanitas Cerro Colorado Formation of the Sierra de Los Condores Group, Province of Cordoba, Argentina. Earth Planet. Sci. Lett. 16, 370–378.

Van der Voo, R., 1993. Paleomagnetism of the Atlantic, Tethys and Iapetus Oceans. Cambridge University Press, Cambridge, U.K.

Van Fossen, M.C., Kent, D.V., 1992. Paleomagnetism of 122 Ma plutons in New England and the mid-Cretaceous paleomagnetic field in North America: true polar wander or large-scale differential mantle motion. J. Geophys. Res. 97, 19651–19661.

Van Fossen, M.C., Kent, D.V., 1993. Palaeomagnetic study of 143 Ma Kimberlite dikes in central New York state. Geophys. J. Int. 113, 175–185.

Wilson, M., Guiraud, R., 1992. Magmatism and rifting in western and central Africa, from Late Jurassic to recent times. Tectonophysics 213, 203–225.

Zijderveld, J.D.A., 1967. A.C. demagnetization of rocks. In: Collinson, D.W., Creer, K.M., Runcorn, S.K. (Eds.), Methods in Paleomagnetism. Elsevier, New York, pp. 256–286.